Ruthenium Nanoparticles: Size, Shape, and Self-Assemblies

G. Viau,*,† R. Brayner,† L. Poul,† N. Chakroune,† E. Lacaze,§ F. Fiévet-Vincent,† and F. Fiévet†

ITODYS UMR 7086, Université Paris 7 Denis Diderot, case 7090, 2 place Jussieu, F-75251 Paris Cedex 05, France, and Groupe de Physique des Solides, UMR 7588, 2 place Jussieu F-75251 PARIS Cedex 05, France

Received May 22, 2002. Revised Manuscript Received November 4, 2002

Ruthenium nanoparticles were prepared by reduction of $RuCl_3$ in a liquid polyol. The mean particle size was restricted to the 1−6 nm range by appropriate choice of the reduction temperature and the acetate ion concentration in the solution. Very narrow particle diameter distributions were obtained. In some samples, among nearly isotropic particles, platelets with aspect ratios as low as 1/4 were detected. Colloidal solutions in toluene were obtained by coating the metal particles with dodecane thiol. Self-assemblies of 4-nm-sized coated particles were studied on a transmission electron microscope grid. The dodecane thiol concentration in the colloidal solution was found to determine, within the particle monolayer, the formation of either columnar units made up of edgewise stacked platelets, or a hexagonal network with a mean distance between the particles of 2 nm. The stacking of hexagonal arrays of particles was also studied, and both closed-packed and noncompact stackings were found. In the noncompact stacking, moiré images resulted from the twisting of the two hexagonal layers with respect to each other. Reconstructions of moiré patterns were observed to favor the 6-fold and 2-fold sites.

1. Introduction

Fine metal particles in the nanometer size range find numerous applications in different fields such as catalysis, electronics, optics, and magnetism. Several studies have shown that thousand- and hundred-atom transition metal clusters present electronic and magnetic properties that differ markedly from those of bulk materials.[1] Because most physical and chemical properties depend on the size and shape of the solid particles, their use as advanced materials in high technology or as model materials in fundamental studies requires nonagglomerated, uniform particles with a controlled mean size and a narrow size distribution. Different physical, chemical, or electrochemical methods have been used in order to obtain uniform metal powders. Among them, chemical methods, particularly the reduction of metal salts in homogeneous solution,[2] in two liquid-phase systems,[3] or in reverse micelles[4] have been used to prepare well-defined mono- and bimetallic[5] particles. Metal can also be produced in solution by decomposition of a zerovalent precursor such as a metal carbonyl or organometallic complexes.[6] Control of particle size is attained through the control of the nucleation and growth steps by acting upon several parameters, such as the nature of the reducing agent and the nature and amount of surfactant or protective agent.[7] In most cases, the metal particles prepared by liquid-phase processes present an isotropic shape. Nevertheless, in some cases cubic or acicular shapes were obtained by using a surfactant or protective agent which bonds preferentially to one metal crystallographic plane, inducing oriented growth.[8]

Moreover, ordered 1D, 2D, or 3D nanoparticle superlattices have been the subject of intensive work the past few years. These superlattices are obtained by either self-assembly of particles coated with alkyl chains,[9] or by assembling particles upon functionalized surfaces.[10] Nanoparticle networks are of special interest for studying collective electronic properties and dipolar interaction effects on magnetic or optical properties.[11] The

* To whom correspondence should be addressed. E-mail: viau@ccr.jussieu.fr.

† ITODYS.

§ Groupe de Physique des Solides.

(1) (a) Volokitin, Y.; Sinzig, J.; De Jongh, L. J.; Schmid, G.; Vargaftik, M. N.; Moiseev, I. I. *Nature* **1996**, *384*, 621. (b) Cox, A. J.; Louderback, J. G.; Apsel, S. E.; Bloomfield, L. A. *Phys. Rev. B* **1994**, *49*, 12295. (c) Respaud, M.; Broto, J. M.; Rakoto, H.; Fert, A. R.; Thomas, L.; Barbara, B.; Verelst, M.; Snoek, E.; Lecante, P.; Mosset, A.; Osuna, J.; Ould Ely, T.; Amiens, C.; Chaudret, B. *Phys. Rev. B* **1998**, *57*, 2925.

(2) (a) Schmid, G. *Chem. Rev.* **1992**, *92*, 1709. (b) Brown, K. R.; Walter, D. G.; Natan, M. J. *Chem. Mater.* **2000**, *12*, 306.

(3) Brust, M.; Fink, J.; Bethell, D.; Schiffrin, D. J.; Kiely, C. J. *J. Chem. Soc., Chem. Commun.* **1995**, 1655.

(4) (a) Taleb, A.; Petit, C.; Pileni, M. P. *Chem. Mater.* **1997**, *9*, 950. (b) Lisiecki, I.; Pileni, M. P. *J. Phys. Chem. B* **1995,** *99*, 5077.

(5) Toshima, N.; Yonezawa, T. *New J. Chem.* **1998**, 1179.

(6) (a) Duteil, A.; Quéau, R.; Chaudret, B.; Mazel, R.; Roucau, C.; Bradley, J. S. *Chem. Mater.* **1993**, *5*, 341. (b) Pan, C.; Dassenoy, F.; Casanove, M.-J.; Philippot, K.; Amiens, C.; Lecante, P.; Mosset, A.; Chaudret, B. *J. Phys. Chem. B* **1999**, *103*, 10098.

(7) Hosteler, M. J.; Wingate, J. E.; Zhong, C.-J.; Harris, J. E.; Vachet, R. W.; Clark, M. R.; Londono, J. D.; Green, S. J.; Stokes, J. J.; Wignall, G. D.; Glish, G. L.; Porter, M. D.; Evans, N. D.; Murray, R. W. *Langmuir* **1998**, *14*, 17.

(8) (a) Wang, Z. L.; Ahmad, T. S.; El-Sayed, M. A. *Surf. Sci.* **1997**, *380*, 302. (b) Puentes, V. F.; Krishnan, K. M.; Alivisatos, A. P. *Science* **2001**, *291*, 2115.

10.1021/cm0212109 CCC: $25.00
Published on Web 12/13/2002

self-assembly of colloidal particles has been studied mostly with nearly spherical or at least isotropic particles. It leads generally to isotropic assemblies: 2D hexagonal networks and 3D face-centered cubic structures.[12] There has been very little work on the organization of anisotropic particles.[8b] It is well-known that suspensions of rod- or platelike colloidal particles may exhibit several phase transitions, from isotropic to nematic and to columnar phase for platelets,[13] but a complete description of the driving forces that control 2D or 3D anisotropic nanoparticle organizations has not yet been proposed.

In the first part of this paper we report the synthesis of fine ruthenium particles by reduction in a liquid polyol. Reduction of metal salts in liquid polyols has proven to be a suitable method for the synthesis of monodisperse metal particles in the micrometer, submicrometer, and nanometer size range.[14] In this method the liquid polyol acts as solvent for the metal salts, reducing agent, and growth medium for the metal particles. One of the specificities of this process is that the reacting temperature can be adjusted over a very large range owing to high boiling points of the liquid polyols.[15] The case of ruthenium is interesting because it is one of a very few easily reducible transition metals that crystallizes only in a hexagonal compact structure. Most transition metals crystallize in cubic structures for which the absence of single axis makes anisotropic growth in homogeneous solution difficult. We show here that ruthenium nanoparticles can present a platelike shape owing to their hexagonal structure.

Electrostatic stabilization was preferred to steric because noble metal particles prepared in this way present a strong affinity for amino and thiol groups. This allowed the preparation of catalysts by immobilization of polyol-prepared Ru particles on oxide surfaces via amino-silane molecules.[16] The very narrow size dispersion of the samples offered us the additional opportunity to study the self-organization of the metal particles coated with dodecane thiol. Several kinds of organization are reported in the second part of this paper. The conditions for assembling nanosized platelets into either anisotropic units or hexagonal 2D arrays are defined. The stacking of hexagonal arrays of particles was also studied, and both compact and noncompact stackings are reported.

2. Experimental Section

Ruthenium metal particles were prepared by reduction of ruthenium (III) chloride in a liquid polyol. $RuCl_3$ was purchased from Fluka; and sodium acetate trihydrate, 1,2-propane diol, 1,2-ethane diol, and bis(2-hydroxyethyl) ether were purchased from Acros. $RuCl_3$ and $CH_3CO_2Na{\cdot}3H_2O$ were dissolved in 200 mL of diol. The ruthenium chloride concentration was 3.25×10^{-3} mol·L^{-1} in all experiments. The sodium acetate concentration was varied from 1.0×10^{-2} mol·L^{-1} to 1.0×10^{-1} mol·L^{-1}. The polyol solution was heated to a temperature in the range 140−180 °C for 10 min with stirring. In this temperature range the solution turned from intense red to pale green and finally to brown, indicating the reduction. The temperatures required to achieve quantitative reactions within 10 min are 150 °C, 170 °C, and 180 °C, for propane diol, ethane diol, and bis(2-hydroxyethyl) ether, respectively. Metal particles were separated from polyol either by centrifugation or by extraction in toluene solution of alkane thiol. Reactions are considered to be quantitative when the recovered polyol is colorless (a pale green polyol indicates the presence of unreduced Ru(II) species).

Metal particles were prepared in a hydrophilic medium (polyol) and were extracted from this medium into a dodecane thiol solution in toluene. Polyol and toluene are immiscible at room temperature, and migration of the metal particles toward the hydrophobic phase is complete provided that the thiol/Ru molar ratio is high enough, namely higher than 0.1. To favor separation of the two phases, distilled water was added to the polyol. Several colloidal solutions containing coated particles in toluene were prepared; the dodecane thiol concentration was in the $0.5 \times 10^{-4} - 2 \times 10^{-2}$ mol·L^{-1} range, the metal concentration was $0.5 \times 10^{-3} - 2\ 10^{-3}$ mol·L^{-1}, and the thiol/Ru molar ratio varied from 0.1 to 40.

TEM observations were carried out with a JEOL 100 kV JEM-100CX II microscope. One drop of the desired colloidal solution in toluene was deposited on the amorphous carbon membrane of the transmission electron microscope grid and the solvent was then evaporated at room temperature. The mean diameter (d_m), and standard deviation (σ) of the size distribution were estimated from image analysis of ca. 250 particles.

Phase analysis of powder recovered by centrifugation was performed by X-ray diffraction (XRD) using a CGR X-ray powder diffractometer (Co Kα radiation).

3. Results and Discussion

3.1. Ruthenium Particle Characterization. The sample morphology (particle size and degree of agglomeration) was found to depend strongly on the amount of sodium acetate dissolved in the polyol. In the absence of acetate ions, micrometer-size particles with no well-defined shape are formed. For acetate concentrations over 1.0×10^{-2} mol·L^{-1}, agglomeration of metal particles is avoided and nanometer sized particles are obtained whatever polyol is used.

3.1.1 Size Control. When 1,2-propane diol was used, the metal particle size was restricted to the nanometer

(9) (a) Whetten, R. L.; Khoury, J. T.; Alvarez, M. M.; Murthy, S.; Vezmar, I.; Wang, Z. L.; Stephens, P. W.; Cleveland, C. L.; Luedtke, W. D.; Landman, U. *Adv. Mater.* **1996**, *8*, 428. (b) Kiely, C. J.; Fink, J.; Brust, M.; Bethell, D.; Schiffrin, D. J. *Nature* **1998**, *396*, 444. (c) Chung, S.-W.; Markowitch, G.; Heath, J. R. *J. Phys. Chem. B* **1998**, *102*, 6685. (d) Motte, L.; Pileni, M. P. *J. Phys. Chem. B* **1998**, *102*, 4104. (e) Sun, S.; Murray, C. B. *J. Appl. Phys.* **1999**, *85*, 4325. (f) Schmid, G.; Chi, L. F. *Adv. Mater.* **1998**, *10*, 515. (g) Chemseddine, A.; Jungblut, H.; Boulmaaz, S. *J. Phys. Chem. B* **1996**, *100*, 12546. (h) Petit, C.; Taleb, A.; Pileni, M. P. *J. Phys. Chem. B* **1999**, *103*, 1805. (i) Gomez, S.; Phillipot, K.; Collière, V.; Chaudret, B.; Senocq, F.; Lecante, P. *Chem. Commun.* **2000**, 1945.

(10) (a) Freeman R. G.; Grabar, K. C.; Allison, K. J.; Bright, R. M.; Davis, J. A.; Guthrie, A. P.; Hommer, M. B.; Jackson, M. A.; Smith, P. C.; Walter, D. G.; Natan, M. J. *Science* **1995**, *267*, 1629. (b) Schmid, G.; Bäumle, M.; Beyer, N. *Angew. Chem., Int. Ed.* **2000**, *39*, 181. (c) Sato, T.; Brown, D.; Johnson, B. F. G. *Chem. Commun.* **1997**, 1007.

(11) (a) Kim, S.-H.; Medeiros-Ribeiro, G.; Ohlberg, D. A. A.; Stanley Williams, R.; Heath, J. R. *J. Phys. Chem. B* **1999**, *103*, 10341. (b) Legrand, J.; Petit, C.; Bazin, D.; Pileni, M. P. *Appl. Surf. Sci.* **2000**, *164*, 193.

(12) (a) Motte, L.; Billoudet, F.; Lacaze, E.; Douin, J.; Pileni, M. P. *J. Phys. Chem. B* **1997**, *101*, 138. (b) Korgel, B. A.; Fullam, S.; Connolly, S.; Fitzmaurice, D. *J. Phys. Chem. B* **1998**, *102*, 8379.

(13) Van der Kooij, F. M.; Van der Beek, D.; Lekkerkerker, H. N. W. *J. Phys. Chem.* **2001**, *105*, 1696.

(14) (a) Fiévet, F.; Lagier, J.-P.; Blin, B.; Beaudouin, B.; Figlarz, M. *Solid State Ionics* **1989**, *32/33*, 198. (b) Ducamp-Sanguesa, C.; Herrera-Urbina, R.; Figlarz, M. *J. Solid State Chem.* **1992**, *100*, 272. (c) Viau, G.; Fiévet-Vincent, F.; Fiévet, F. *J. Mater. Chem.* **1996**, *6*, 1047. (d) Toneguzzo, P.; Viau, G.; Acher, O.; Fiévet-Vincent, F.; Fiévet, F. *Adv. Mater.* **1998**, *10*, 1032.

(15) Fiévet, F. In *Fine Particles: Synthesis, Characterization, and Mechanism of Growth;* Surfactant Science Series, Vol. 92; Sugimoto, T., Ed.; Marcel Dekker: New York, 2000; p 460.

(16) Brayner, R.; Viau, G.; Bozon-Verduraz, F. *J. Mol. Catal. A* **2002**, 3465.

Table 1. Dependence of the Mean Diameter (d_m) and Size Distribution (σ) of Ruthenium Particles Prepared by Reduction of $RuCl_3$ in 1,2-Propane Diol on the Temperature and Acetate Ion Concentration (Ru Concentration = 3.25 10^{-3} Mol·L^{-1})

reaction time (min)	T (°C)	acetate (mol·L^{-1})	d_m (nm)	σ (nm)	σ/d_m
10	165	1.1×10^{-2}	1.6	0.24	0.15
10	165	2.2×10^{-2}	1.4	0.18	0.13
10	165	4.4×10^{-2}	1.8	0.18	0.10
10	150	1.0×10^{-2}	3.95	0.26	0.066
10	150	2.0×10^{-2}	1.7	0.21	0.12
10	150	4.0×10^{-2}	2.0	0.25	0.125
10	150	8.8×10^{-2}	2.5	0.28	0.11
30	140	1.0×10^{-2}	6		
30	140	2.0×10^{-2}	2.2		

range by selecting the acetate concentration and the synthesis temperature (Table 1). Whatever the acetate concentration, the particles are smaller when the temperature increases. For a given temperature the particle diameter does not vary steadily with the acetate concentration. In every case the size distribution is very narrow, with a standard deviation less than 15% of the mean diameter (Figure 1). Thus the polyol process offers the opportunity to prepare monodisperse ruthenium particles reproducibly with a mean diameter in the 1.5−6 nm range. It must be stressed that the very low standard deviation of the 4 nm-sized particles is obtained on the whole sample without any size selection processes often used in order to obtain monodisperse samples.

The general scheme for formation of metal particles by reduction of a metallic salt in a liquid polyol is as follows: dissolution of the precursor, reduction of the dissolved species, nucleation, and growth from the solution.[14a,15] The preparation of monodisperse particles requires control of the nucleation and growth steps. In such a liquid-phase process, noble metal particles have a strong tendency to coalesce during their formation. Polymers, especially poly(vinylpyrrolidone) (PVP), have been used by several groups as protective agents in polyols to avoid particle agglomeration.[17,18] Electrostatic stabilization is an alternative way to obtain colloidal particle dispersions in solution. Anions, namely citrate ions, are generally used for aqueous colloidal solutions of silver, gold, and platinum.[2b,19] Added in sufficient amount, acetate ions, as opposed to chloride or hydroxide ions,[20] were found to permit the formation of nonagglomerated ruthenium particles in polyols. This means that acetate ions present a strong affinity for ruthenium metal particles and provide them a high enough zeta potential to prevent agglomeration. It must be noted that Ru is not the only metal that can be prepared as nonagglomerated nanoparticles in acetate solutions in polyols. It is also the case for platinum, rhodium, and iridium.[21]

Two parameters were found to determine the particle size: the temperature and the acetate concentration.

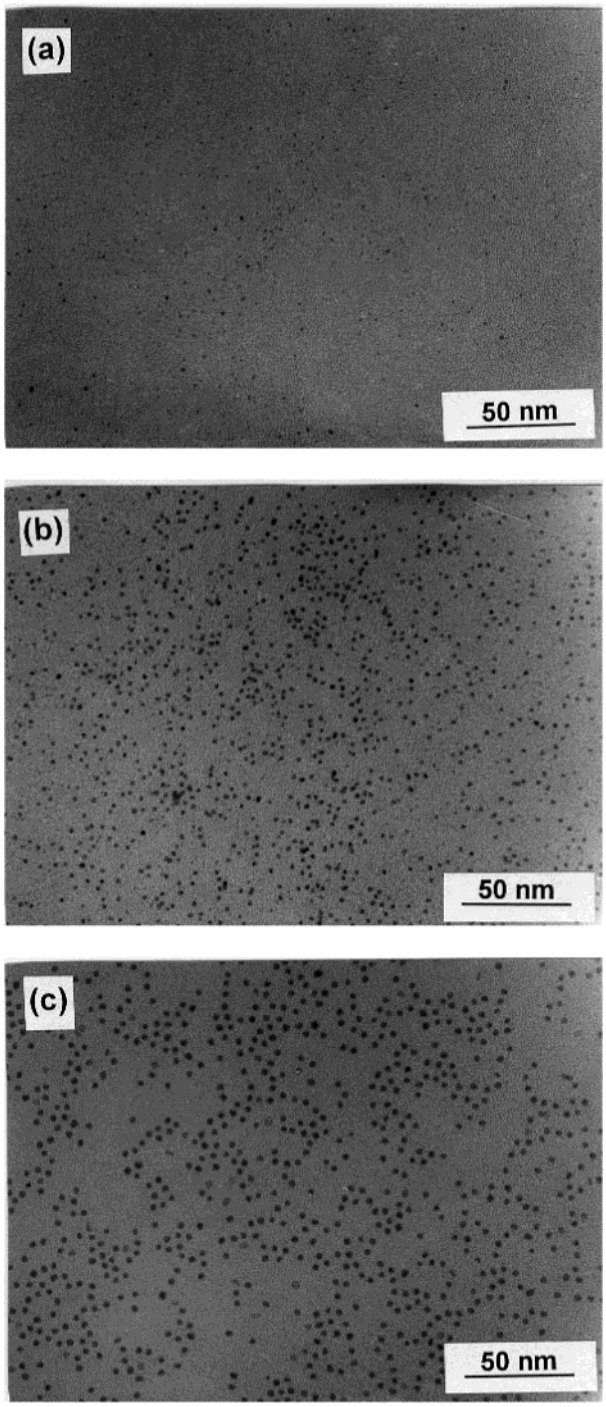

Figure 1. Transmission electron microscopy image of ruthenium particles prepared in sodium acetate solution in 1,2-propane diol: (a) $d_m = 1.4$ nm; (b) $d_m = 2.5$ nm; and (c) $d_m = 3.5$ nm.

Decreasing the particle size by increasing the temperature of reduction was previously observed for other metals in polyol.[14a] The higher the temperature, the higher is the nucleation rate, and, for a given concentration of metal, the lower is the mean particle size. The dependence of the mean size on the acetate concentration is rather more complex to interpret because acetate ions can act as ligands for both the metal particles and the Ru(III) and Ru(II) species in solution. Smaller particles can be expected when the acetate concentration increases, as it allows high surface charge of the metal particles. On the other hand, a high acetate/Ru

(17) Silvert, P. Y.; Herrera-Urbina, R.; Duvauchelle, N.; Vijayakrishnan, V.; Tekaia-Elhsissen, K. *J. Mater. Chem.* **1996**, *6*, 573.
(18) Toshima, N.; Lu, P. *Chem. Lett.* **1996**, 729.
(19) Turkevitch, P. C. *Gold Bull.* **1985**, *18*, 86.
(20) Miyazaki, A.; Takeshita, K.; Aika, K. I.; Nakano, Y. *Chem. Lett.* **1998**, 361.
(21) Viau, G.; Toneguzzo, P.; Pierrard, A.; Acher, O.; Fiévet-Vincent, F.; Fiévet, F. *Scripta. Mater.* **2001**, *44*, 2263.

ratio can probably reduce the rate of reduction by stabilizing the oxidized species and hence decreasing the nucleation rate. The dependence of the mean particle size on the amount of acetate ion in solution may be related to these two contradictory effects.

3.1.2 Particle Shape. TEM images provide us a 2D representation of objects. Metal particles were described above as equi-axed particles, as is generally the case for particles, including those of ruthenium,[20,22] prepared by wet chemistry processes. Nevertheless, for samples consisting of 4-nm-sized particles, a significant number of particles were found to deviate from an isotropic shape (Figure 2a). Particles with aspect ratios as low as 1/4 were observed in some conditions. It is noteworthy that these particles are rarely found isolated but are generally assembled with other anisotropic particles. More details about such assemblies will be given in the next section.

At first sight, particles with an aspect ratio of 1/4 can be described as rodlike (1 nm × 4 nm). High-resolution microscopy showed that the crystallographic *c*-axis is perpendicular to the major axis of the particles (Figure 2b) which suggests that they are hexagonal platelets rather than acicular particles, in accordance with their structure (cf. next section). For a hcp single crystal the Wulf polyhedron is a truncated hexagonal bipyramid.[23] The anisotropy of the crystal is related to the thickness and the diameter of the bipyramid. Assuming that the *c* parameter is the same as that of bulk ruthenium (c = 0.42819 nm), the observed thickness of 1 nm corresponds to six atomic layers.

In fact, the morphological aspect of a sample was found to depend on the dodecane thiol concentration of the colloidal solution prepared for TEM observations. Two colloidal solutions were prepared with the same particles and containing dodecane thiol at 0.5×10^{-4} mol·L^{-1} and 2×10^{-2} mol·L^{-1}, respectively. The thiol/Ru ratio was 0.1 in the former solution and 40 in the latter. The experimental conditions for the observation of anisotropic particles were fulfilled only when the thiol/Ru ratio was very low (Figure 2a). For the high thiol/Ru ratio solution, anisotropic particles cannot be detected on the TEM image over very large areas (Figure 2c), which means that all the particles are viewed sideways. This confirms that the anisotropic particles are indeed platelets and not nanorods, and decreasing the amount of thiol in the solution favors the edgewise orientation of the platelets.

In some samples, particles with an aspect ratio lying in the 1/4−1/2 range represent about 15% of the total number, while 85% present an aspect ratio close to 1 and can be considered as isotropic. The distribution of the particle thickness is nevertheless a rough estimate, because it is not certain that all the platelets are viewed edgewise in the TEM image. On the other hand, the diameter distribution can be inferred from Figure 2c and is found to be very narrow.

3.1.3 X-ray Diffraction. The particles recovered by centrifugation are crystalline, as shown by XRD (Figure

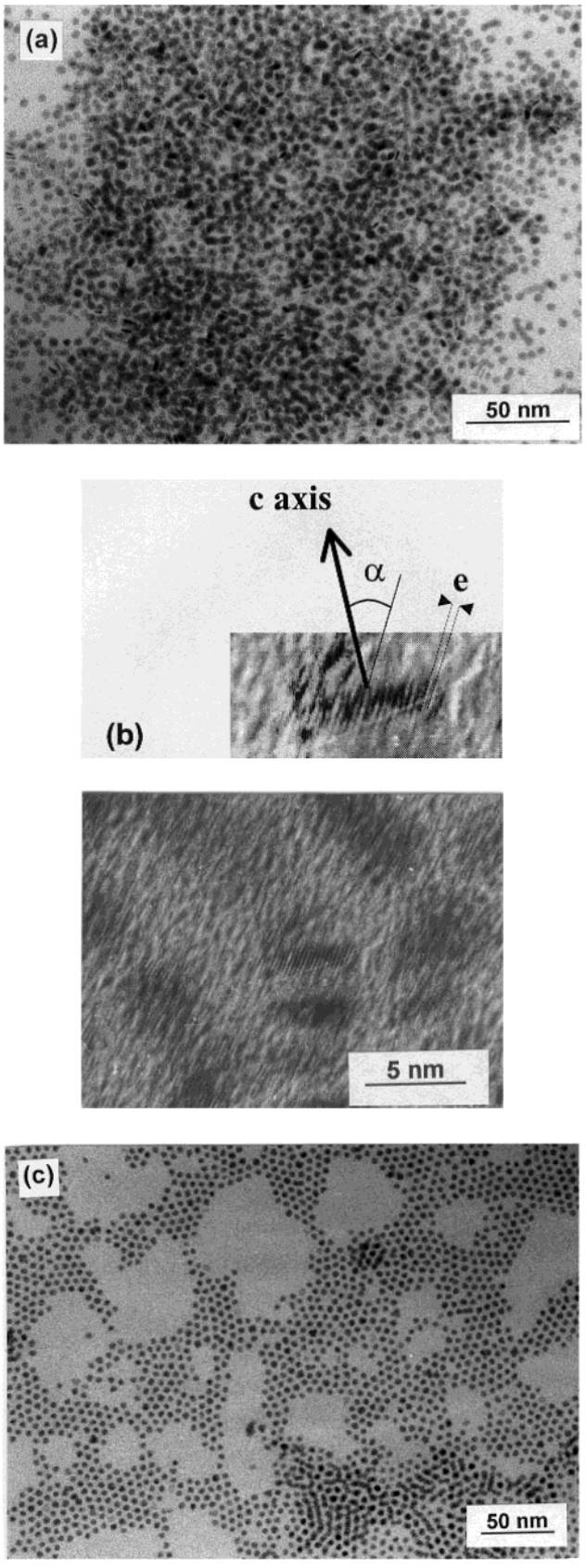

Figure 2. (a) TEM image of 4-nm mean diameter ruthenium particles with dodecane thiol (thiol/Ru = 0.1); (b) High-resolution TEM image of a representative anisotropic ruthenium particle: e = 2.05 Å corresponds to the (10.1) inter-planar distance, $\alpha = 28.7°$ is the angle between the (10.1) plane and the *c* axis; (c) TEM image of the same 4-nm ruthenium particles with a large excess of dodecane thiol (thiol/Ru = 40).

(22) (a) Vidoni, O.; Philippot, K.; Amiens, C.; Chaudret, B.; Balmes, O.; Malm, J.-O.; Bovin, J.-O.; Senocq, F.; Casanove, M.-J. *Angew. Chem., Int. Ed.* **1999**, *38*, 3736. (b) Gao, S.; Zhang, J.; Zhu, Y.-F.; Che, C.-M. *New J. Chem.* **2000**, *24*, 739.

(23) Kitakami, O.; Sato, H.; Shimada, Y.; Sato, F.; Tanaka, M. *Phys. Rev. B* **1997**, *56*, 13 849.

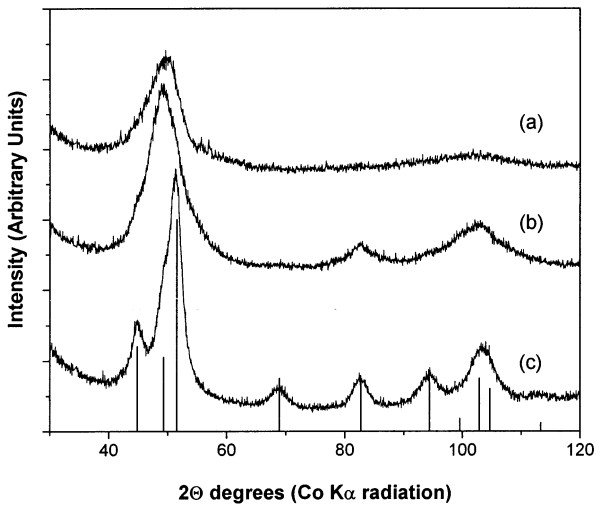

Figure 3. XRD pattern (Co Kα radiation) of Ru powders obtained by reduction of $RuCl_3$ in 1,2-propane diol: (a) 2.5-nm-sized particles; (b) 4-nm-sized particles; and (c) agglomerated particles prepared without acetate ions.

3). Their pattern can be indexed as a hcp lattice as expected for ruthenium metal particles.[24] For small particles X-ray line broadening becomes important. The full width at half-height is found to depend on the (*hkl*) indexes, which suggests that there are stacking faults or anisotropic crystals. Nevertheless, because of the considerable broadening it was not possible to clearly establish the major contribution.

3.2. Ruthenium Particle Self-Assemblies. Particles with a diameter of 4 nm and coated with dodecane thiol were studied in more detail because we observed that smaller particles self-organized with more difficulty. Particle self-assemblies are partly controlled by the van der Waals attraction energy between particles. For spherical particles this energy is proportional to the particle radius.[25] For very fine particles the attraction is weak and is counterbalanced by other interactions, which explains their lesser ability to self-organize.

Several colloidal solutions containing coated particles in toluene were prepared with different dodecane thiol and metal concentrations and thiol/Ru molar ratios. By varying the metal concentration, the particle density on the TEM grid was varied from less than a monolayer to multilayers. By varying the thiol/Ru ratio over 2 orders of magnitude the nature of the colloidal solution was changed.

For 4-nm-sized particles the number of metal atoms at the surface of the particles can be estimated to be 25−30% of the total number of atoms in the particle, depending on the shape.[26] On a gold (111) surface, the thiol density corresponds to a thiol/Au surface ratio of 33%. Higher thiol densities are found on nanoparticles, in the 45−60% range for the thiol/surface metal atom, depending on the particle size.[27] Thus, a rough calculation shows that a thiol/total Ru atom ratio of 0.1 corresponds to an amount of dodecane thiol slightly lower than the minimum necessary to achieve a complete coating of the 4-nm-sized particles. For molar ratios higher than ca. 0.2 dodecane thiol is present in excess in the solution and a very large amount of free thiol is present in solution for a molar ratio of 10.

It has been established that the formation of either 2D monolayers or 3D aggregates of particles coated with alkyl chains on a substrate depends on several parameters, such as the chain length,[28] the interparticle attraction, the solvent polarity,[29] and the nature of the substrate.[30] In our case, the drop of toluene solution spread out quite well on the microscope grid and 3D particle aggregates were not observed. Several patterns of organization on the TEM grid were observed, depending on the dodecane thiol concentration and on the particle density. Results are presented below, first for dilute Ru colloidal solutions and then for solutions where bilayer organizations of the particles on the grid could be observed.

3.2.1 Dilute Solutions. We showed in Section 3.1.2 that for a high thiol/Ru solution, anisotropic particles cannot be distinguished on the TEM image (Figure 2c). Moreover, the particles are ordered in a hexagonal network with a mean distance between the particles of 2 nm. Such hexagonal networks are obtained provided that there is enough thiol. The interparticle spacing is then independent of the thiol concentration of the solution, particularly when there is excess thiol. These hexagonal arrays are very similar to those obtained previously with spherical silver[4a,31] or Ag_2S[32] particles of the same mean diameter and coated with alkyl chains. The distance of 2 nm is shorter than twice the length of the alkyl chain in an all-trans conformation; it shows that the dodecane thiol chains are interdigitated. The similarity with distances measured with other kinds of particle shows that the energy balance is basically the same as in the other self-organized patterns of metal particles such as silver or gold. This suggests that the Hamaker constant expressing the van der Waals attraction between the particles is roughly of the same order of magnitude for ruthenium, gold, and silver. As mentioned in a previous section, the distribution on the particle aspect ratio is not known with accuracy. Clearly the presence of a small number of thin platelets does not perturb the hexagonal array of the monolayer.

The experimental conditions for the TEM observation of anisotropic particles were described in Section 3.1.2: a significant number of platelike particles are viewed edgewise for low thiol/Ru solutions. Furthermore, the platelets are almost never observed isolated but are usually stacked in lines lying over the grid and made up of a few particles sharing their *c* axis (Figure 4a). In these units the mean distance between the particle sides is 1 nm. This is much lower than the interparticle distance in the hexagonal network and it is too short to be compatible with adsorbed dodecane thiol in an all-

(24) X-ray powder data file JCPDS n*o*. 06-0663.
(25) Israelachvili, J. *Intermolecular and Surface Forces*, 2nd ed.; Academic Press: London, 1992; p 176.
(26) Van Hardeveld, R.; Hartog, F. *Surf. Sci.* **1969**, *15*, 189.
(27) (a) Badia, A.; Cuccia, L.; Demers, L.; Morin, F.; Bruce Lennox, B. *J. Am. Chem. Soc.* **1997**, *119*, 2682. (b) Hosteler, M. J.; Stokes, J. J.; Murray, R. W. *Langmuir* **1996**, *12*, 3604.
(28) Motte, L.; Pileni, M. P. *J. Phys. Chem. B* **1998**, *102*, 4104.
(29) Korgel, B. A.; Fitzmaurice, D. *Phys. Rev. Lett.* **1998**, *80*, 3531.
(30) Motte, L.; Lacaze, E.; Maillard, M.; Pileni, M. P. *Langmuir* **2000**, *16*, 3803.
(31) Harfenist, S. A.; Wang, Z. L.; Alvarez, M. M.; Vezmar, I.; Whetten, R. L. *J. Phys. Chem. B* **1996,** *100*, 13904.
(32) Motte, L.; Billoudet, F.; Lacaze, E.; Pileni, M. P. *Adv. Mater.* **1996**, *8*, 1018.

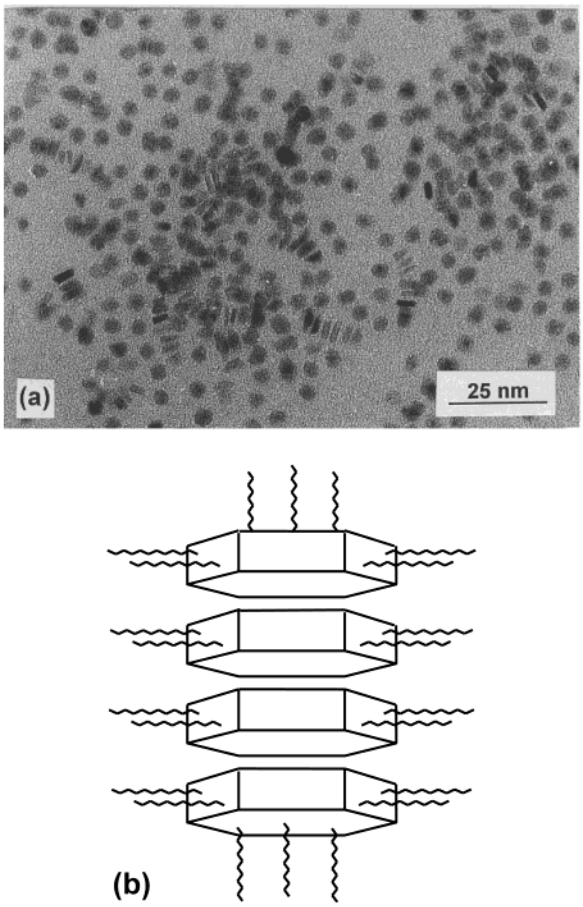

Figure 4. (a) TEM images of lines consisting of a few platelet particles; (b) schematic representation of a line.

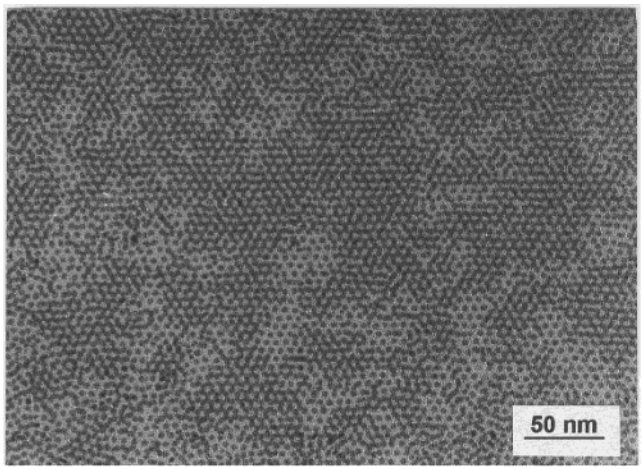

Figure 5. TEM image of 4-nm-sized Ru particles mono- and bilayer showing compact stacking.

trans conformation on the particle sides. It shows that no thiol molecules are coated on the large faces of the particles located inside the lines; these particles are not totally coated by dodecane thiol. Thus, for a low thiol concentration: (i) the thiol molecules are preferentially bonded to the particle edge rather than to the dense (00.1) planes that constitute the platelets sides; and (ii) the association of a few particles into anisotropic units is the best way to form hydrophobic units stable in toluene. A representation of these units is proposed in Figure 4b. It is, therefore, highly probable that these units are present in solution and are not the result of a

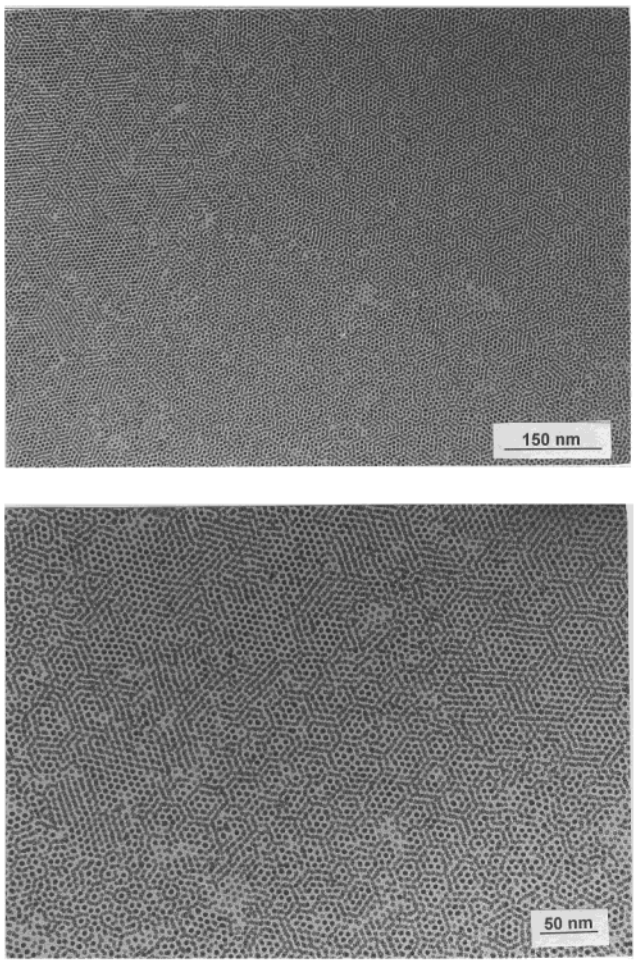

Figure 6. TEM images of 4-nm-sized Ru particles bilayer showing noncompact stacking.

self-assembly process upon the microscope grid. It is interesting to note that directional assembly of anisotropic particles into nanowires was described for silver prolate nanocrystals by Korgel and Fitzmaurice.[33] In that study, the lack of thiol on the particle surface was already suggested as the driving force for the formation of wires. To the best of our knowledge, we present here the first example of the anisotropic assembly of oblate metal nanoparticles.

3.2.2 Organization of the Bilayers. For a metal concentration close to 1×10^{-3} mol·L^{-1} a high coverage ratio on the TEM grid is obtained with the formation of mono- and bilayers. The nature and degree of organization is found to depend on the thiol concentration in the toluene solution. For very low thiol concentration, particles appeared to be poorly organized. Provided that the thiol concentration is higher than 2×10^{-4} mol·L^{-1}, which corresponds to a complete coating of the particles, a very good particle organization with mono- and bilayers of coated particles is observed over a very large area (> 1 μm^2).

As regards the bilayers, various patterns were inferred from TEM observations. The close-packed stacking A−B of the second layer upon the first one, with all the particles of the second layer occupying the 3-fold-sites, was generally observed (Figure 5). Within the first and the second layers the particles are ordered in a

(33) Korgel, B. A.; Fitzmaurice, D. *Adv. Mater.* **1998**, *10*, 661.

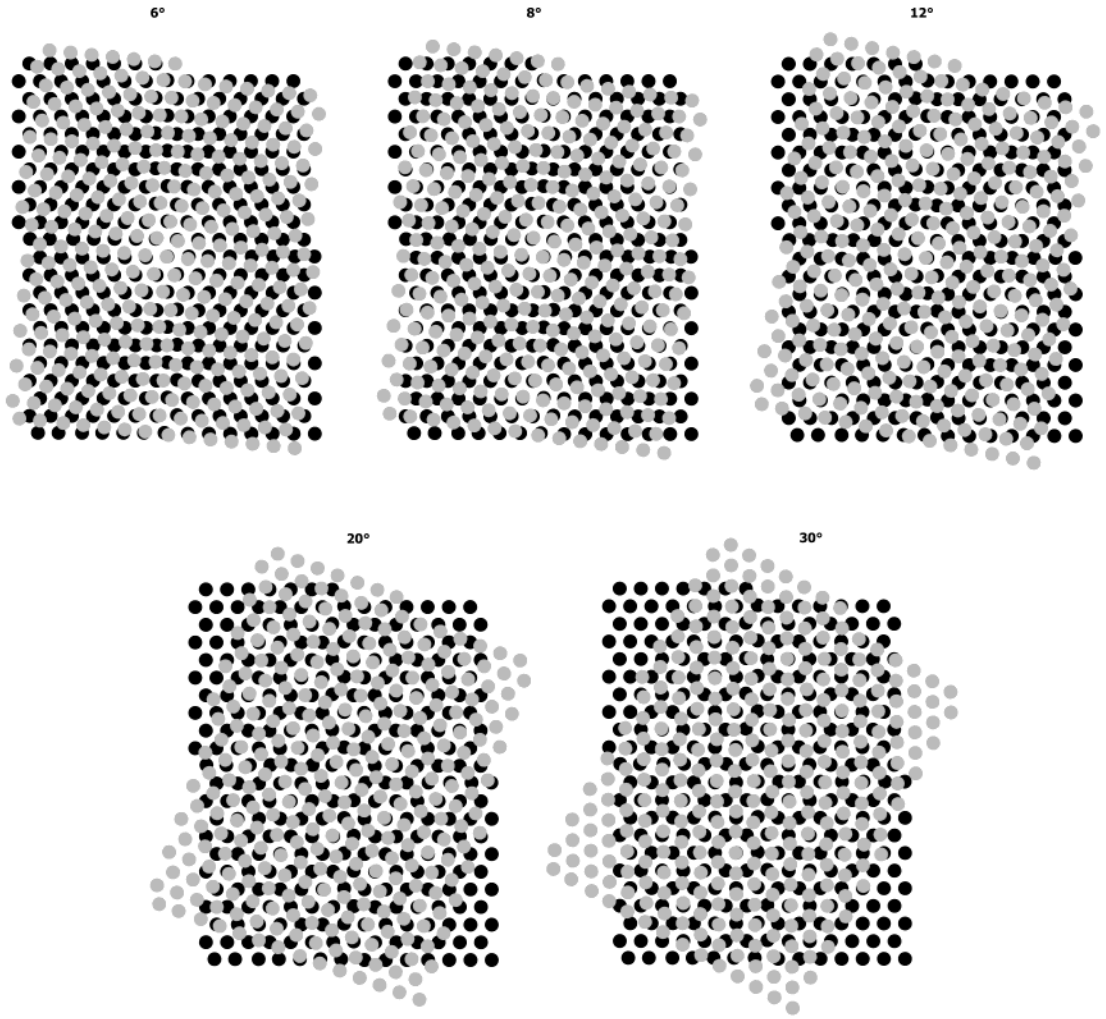

Figure 7. Moiré images obtained by twisting the upper hexagonal layer with respect to the basal one, at different angles θ.

hexagonal network with the same mean distance between the particles.

Other patterns were also observed for bilayers (Figure 6). These assemblies are the result of a noncompact stacking of the two layers: only a very small number of particles in Figure 6 occupy the 3-fold sites expected for a close-packed stacking. In a first approach, the patterns of Figure 6 can be reproduced by moiré images. As shown in Figure 7, similar patterns are obtained by twisting the upper hexagonal layer with respect to the basal one. The patterns produced are hexagonal or circular depending on the respective orientation of the two layers. The experimental twist angle θ is found to take values between a few degrees and 30° (Figure 8). The observation of such patterns shows that the hexagonal particle organization is fairly good within the two layers. It shows also that, as in the close-packed stacking of Figure 5, the mean distance between particles is the same within the two layers.

Nevertheless, it is noteworthy that some areas of the TEM image (Figure 6) show deviations from a moiré pattern. As shown in Figure 7, whatever the angle, the rotation of the second hexagonal layer with respect to the first one generates exactly the same number of particles located in the 3-fold, 2-fold, and 6-fold sites. A closer examination of some parts of the TEM image (Figure 6) reveals a larger number of 6-fold and 2-fold sites occupied than 3-fold ones (Figure 8d). Thus, the hexagonal order within the layers seems to be locally modified by directional particle−particle interactions.

Whereas 3D structures of coated particles previously described present generally a fcc stacking,[12] anomalous stacking of bilayers was already reported by several groups.[12b,34,35] Occupation of 2-fold sites leading to linear or circular arrangements on partially filled bilayers was observed. Directional interaction between particles due to particles faceting[12b] was suggested to explain such a situation that does not correspond to the hard-sphere model.

Ugarte et al.[35] showed unambiguously that for coated gold particle multilayers on a carbon membrane, prepared at 80 °C, the interparticle distance is greater in the first layer than in the second and third. This shortening from 2 to 1.7 nm makes the 2-fold sites energetically favorable for the particles of the second layer. This leads to hexagonal patterns over large areas where all the particles belonging to the second layer occupy a 2-fold site. Prepared at room temperature and with another metal, the bilayers presented in this work do not present such a difference of parameter between

(34) Fink, J.; Kiely, C. J.; Bethell, D.; Schiffrin, D. J. *Chem. Mater.* **1998**, *10*, 922.
(35) Zanchet, D.; Moreno, M. S.; Ugarte, D. *Phys. Rev. Lett.* **1999**, *82*, 5277.

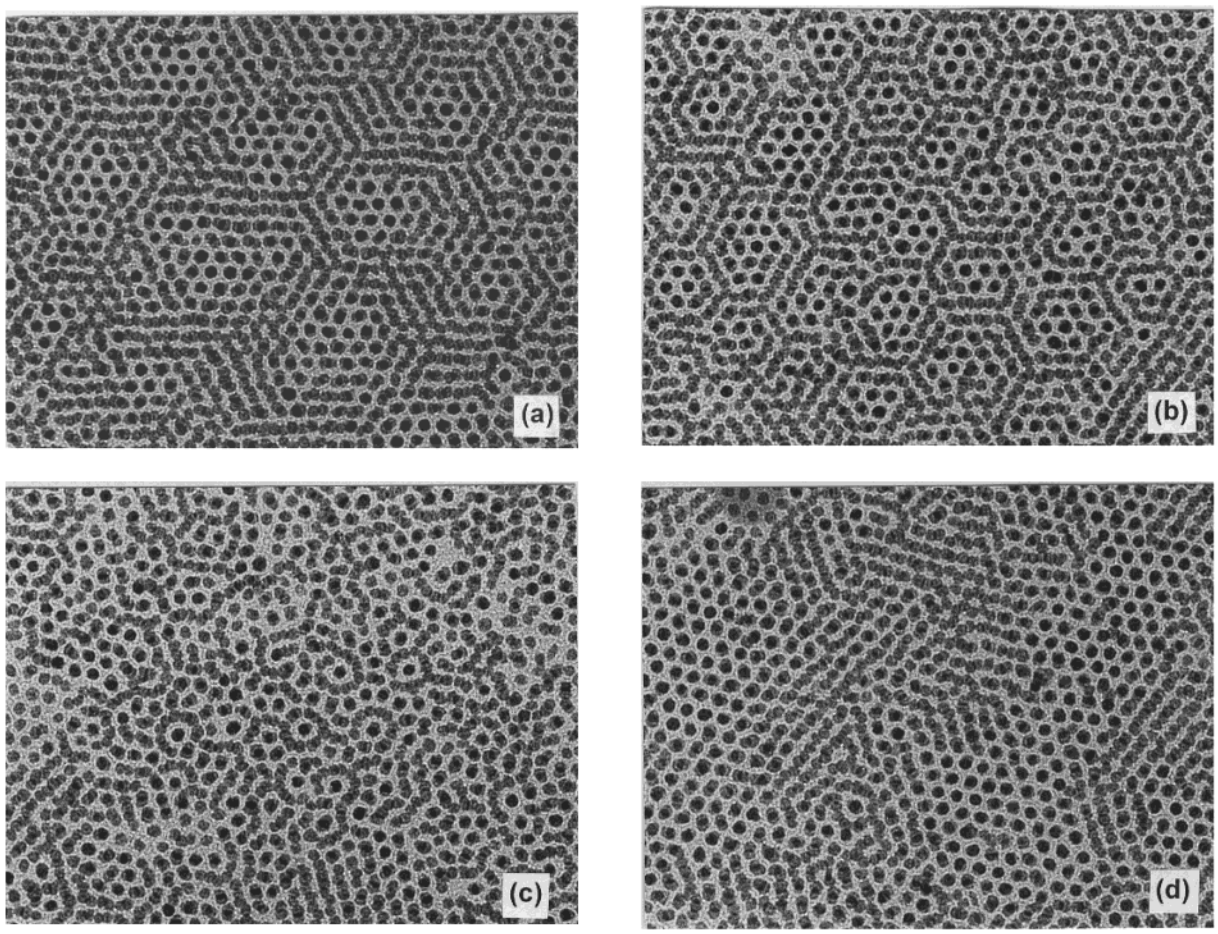

Figure 8. Details of Figure 6 showing: (a), (b), and (c) patterns which can be reproduced by moiré image: (a) $\theta = 8°$; (b) $\theta = 12°$; (c) $\theta = 30°$; and (d) higher 6- and 2-fold sites occupations than expected on the basis of a purely moiré image.

the two first layers, neither in the close-packed stacking (Figure 5) nor in the noncompact stacking (Figure 6). Thus, the influence of the substrate is weaker in the case of Ru nanoparticles probably because the interparticle interaction energy is lower for ruthenium than for gold.

In our case two experimental parameters appear to govern the stacking of the bilayers: the thiol concentration and the particle shape.

We observed that the compact stacking is somewhat favored by high thiol concentration ($>10^{-3}$ mol·L^{-1}), whereas the noncompact stacking is somewhat favored by a lower thiol concentration ($5 \times 10^{-4} - 10^{-3}$ mol·L^{-1}). Moreover, it has been observed that the thiol concentration in toluene modifies both the evaporation rate and the surface tension of the solution. The lower the thiol concentration, the faster the solvent evaporates, and the better the solution drop spreads out on the TEM grid. Thus, at high thiol concentration the particles actually assemble in an excess of thiol and can reach the equilibrium structure, namely the compact stacking. In contrast, when the evaporation time is shorter with a low thiol concentration, particles of the second layer may be frozen in a nonequilibrium state which produces the moiré pattern.

Rotational moiré of hexagonal layers has been observed in layered structures such as (00.1) graphite planes.[36] Moreover, also in case of graphite, local reconstruction of a moiré pattern can take place in order to reach the right location for the greatest number of atoms.[37] What is surprising in the case of Figure 8d is that reconstruction seems to favor the 6-fold or the 2-fold rather than the 3-fold sites. This is probably related to the shape of the particles. We showed in a previous section that under some conditions, in dilute solutions, the anisotropy of the particles could lead to directional assemblies. The distribution of the aspect ratio is not known precisely, but we showed that in some samples the proportion of platelets could reach 15%. Even if this proportion is small, the presence of anisotropic particles will induce a roughness in the first layer and may perturb the stacking of the next one. For particles with an aspect ratio as low as 1/4, the hard-sphere model cannot apply, and for such particles lying on their side, the 6-fold sites are more probably the actual equilibrium location for a particle of the next layer.

In summary, the different patterns observed on bilayers shows close-packed and noncompact stacking which result from different nucleation/growth mechanisms of the second layer upon the first one. It shows also that several sites of the second layer have very similar energies. This work confirms previous results on silver or gold particles for 3- and 2-fold sites and

(36) Kuwabara, M.; Clarke, D. R.; Smith, D. A. *Appl. Phys. Lett.* **1990**, *56*, 2396.
(37) Garbarz, J.; Lacaze, E.; Faivre, G.; Gauthier, S.; Schott, M. *Philos. Mag. A* **1992**, *65*, 853.

extends it to the 6-fold site. Further experimental work must be carried out in order to control accurately the platelet thickness distribution to confirm the influence of the particle shape on their organization.

4. Conclusion

Nonagglomerated ruthenium particles were obtained by reduction in a liquid polyol. The particles crystallize with the expected hcp structure. Experimental conditions were found to control accurately the particle diameter in the nanometer size range with very small standard deviation. Among a majority of isotropic particles, a significant number of particles were found to be platelets, but the thickness distribution was not easily inferred from TEM observations.

The organization of particles coated with dodecane thiol on the carbon membrane of the TEM grid was found to depend on the thiol concentration in the solution.

For very low thiol concentrations, columnar units made up of edgewise stacked platelets are formed. The low coating ratio was showed to be responsible for this directional assembly. Although nematic and smectic phases have already been observed with rodlike shaped nanoparticles, this appears to be the first time that columnar units with disk-shaped metal particles are described and precisely characterized.

For higher thiol concentrations platelets are viewed sideways, and hexagonal arrays of isotropic particles with a mean interparticle distance of 2 nm were observed. Closed-packed and noncompact stacking of two hexagonal layers were evidenced. The first one is favored by a low evaporation rate and probably by a low number of platelets within the sample. Misorientation of the second layer producing moiré patterns was found to be favored by a high evaporation rate. In both cases, the interparticle distance was found to be equal within the first and second layers. The reconstructions of moiré patterns favoring the 6-fold sites observed in some cases were assumed to be related to the presence of anisotropic particles in the samples.

Our better understanding of the directional assembly of platelets either in 1D wires or in 3D stacking encourages us to further investigate the synthesis conditions that control platelet formation in order to obtain well-defined anisotropic organizations.

CM0212109